Path dependent microstructure orientation during strain compression of semicrystalline block copolymers

P.L. Drzal[a], J.D. Barnes[b], P. Kofinas[a],*

[a]*Department of Materials and Nuclear Engineering, University of Maryland, College Park, MD 20742-2115, USA*
[b]*Polymer Structure and Mechanics Group, National Institute of Standards and Technology, Bldg 224, Rm A209, Gaithersburg, MD 20899, USA*

Abstract

The shear-induced morphologies produced by channel die processing of a semicrystalline ethylene/ethylene–propylene/ethylene (E/EP/E) block copolymer were investigated as a function of processing conditions. The microphase separation of the block constituents under the processing conditions used in this work leads to a lamellar stack morphology, referred to as the B population, whose dimensions are controlled by the block molecular masses. In addition, the crystallizable part of the E polymer forms lamellar stacks which are referred to as the C population. The orientation textures of these two lamellar populations depend upon processing conditions in a complex manner. Two-dimensional small angle X-ray scattering (SAXS) was used to determine the domain spacing and orientation of the B and C populations relative to the process directions. The rate at which the channel die assembly was cooled following compression was found to strongly affect the microstructure of the end product. Using a cooling rate of 0.27°C/s, a predominantly perpendicular to the direction of shear orientation of B lamellar populations (B_p) is produced, while a cooling rate of 3.50°C/s yields a predominantly transverse to the direction of shear orientation of C lamellar populations (C_t). Both lamellar microstructures are oriented normal to the plane of shear. This C_t microstructure is novel to semicrystalline block copolymers and is attributed to deformation of preexisting crystallites. © 2001 Elsevier Science Ltd. All rights reserved.

Keywords: Plane strain compression; Block copolymers; Lamellar population

1. Introduction

Block copolymers are macromolecules composed of sequences or blocks of chemically distinct repeat units. The chemical link between different blocks prevents phase separation on a macroscopic length scale. Microphase separation of diblock copolymers leads to spherical, cylindrical, bi-continuous, and lamellar morphologies [1,2]. Although we refer to this microphase-separated structure of block copolymers as microdomains, typical domain sizes are in the nanometer range. These nanostructures are essentially monodisperse, and the morphology and domain sizes can generally be controlled by adjusting the length of each block and the total molecular mass.

Microphase separation can also occur due to crystallization of one or more of the block sequences. Block copolymers containing one or more semicrystalline blocks offer a much wider range of possibilities than wholly amorphous materials with regard to increased toughening, resistance to solvents and acids, and higher working temperature applications. Along with these advantages, incorporating crystallinity into a new material presents a variety of challenging problems, both from a synthesis and a processing point of view. The synthetic pathways required to produce semicrystalline polymers are generally more complex than for wholly amorphous systems, and the interaction between the crystallization and the microphase separation processes has become a topic of several research efforts [3–7].

It is becoming increasingly apparent that processing a single block copolymer material in various flow patterns can lead to a variety of morphologies in the final product depending upon the processing conditions employed. Winey and coworkers have discussed the parallel, perpendicular, and other more complex orientations that are achievable in the case of lamellar systems [8–11]. The behavior of a block copolymer with at least one crystallizable moiety is particularly interesting because of the multiplicity of "frozen-in" morphologies which can be expected [12,13]. Shear-induced morphologies produced above the E block melting point in a series of ethylene/ethylene–propylene (E/EP) diblock and E/EP/E triblock copolymer systems have been

---

* Corresponding author. Tel.: +1-301-405-7335; fax: +1-301-314-2029.
E-mail address: kofinas@eng.umd.edu (P. Kofinas).

reported [14,15], and were attributed to the proximity of the order disorder temperature (ODT) to the processing temperature.

The microphase separation of the E and EP block constituents under the processing conditions used in this work leads to a lamellar stack morphology whose dimensions are controlled by the block molecular masses. This population of lamellae is hereinafter referred to as the *B* population. In addition, the crystallizable part of the E polymer forms lamellar stacks which are hereinafter referred to as the *C* population. We use two-dimensional small-angle X-ray scattering (SAXS) to characterize orientations of these microstructures produced from variations in channel die plane strain compression processing. A novel to semicrystalline block copolymers, transverse to the direction and normal to the plane of shear microstructure orientation is reported in a E/EP/E semicrystalline triblock copolymer system. The ability to control the type and degree of microstructure orientation allows the construction of block copolymer membranes exhibiting anisotropic gas transport properties [16,17].

2. Experimental

2.1. Materials

The E/EP/E 30/40/30 triblock copolymer was synthesized by hydrogenation of 1,4-poly (butadiene)/1,4-poly (isoprene)/1,4-poly (butadiene) (PB/PI/PB) precursor triblocks of molecular masses 30,000, 40,000 and 30,000 g/mol, respectively [14]. The butadiene block consists of 10% 1,2, 35% *trans* 1,4 and 55% *cis* 1,4 PB, while the isoprene block contains 93% *cis* 1,4 and 7% 3,4 PI. The hydrogenated PB block thus resembles low density polyethylene (E) and the hydrogenated PI block is essentially perfectly alternating ethylene propylene rubber (EP). The molecular masses of each block were determined from gel permeation chromatography (GPC) measurements on the polydiene precursors, from knowledge of reactor stoichiometry and conversion, and from a previous demonstration [20] that little or no degradation occurs during the hydrogenation reactions.

2.2. Channel die processing

Isotropic samples were heated to 150°C, above the order disorder transition temperature, to erase any thermal history, in a standard laboratory press equipped with digitally controlled heating platens. Load was applied and released to press the sample into a thin sheet. The heat was turned off and the film was allowed to cool to room temperature. Once cooled, the polymer sheet was cut into 1/2 in. by 1/2 in. squares. The squares were stacked in the center of a 6 by 1/2 in. channel die. The channel die [14,18,19] was placed into the press and heated to the desired temperature, and the polymer was subjected to plane strain compression.

A representation of the channel die and its principal
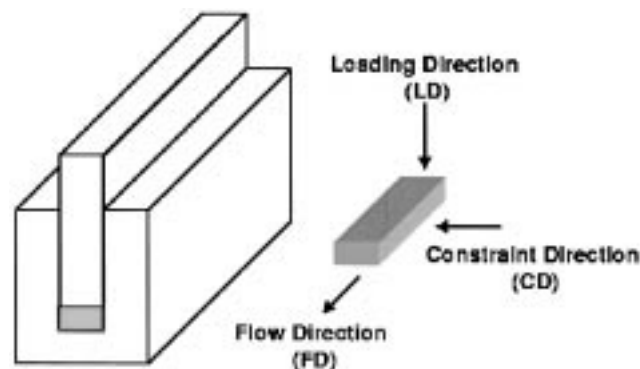

Fig. 1. A representation of the channel die and its three principal deformation directions.

deformation directions, the loading, constraint and flow directions, are shown in Fig. 1. The channel die was maintained at a selected constant temperature during the compression flow. An applied load of 9.2 MPa was maintained continuously using the press, and the polymer was observed to flow from the center outwards, towards the two ends of the channel. The compressed specimens were then quenched under load to room temperature. After the sample was cooled to room temperature, the load was released. The final compression ratio was determined from the reduction of the thickness of the samples. The channel die experiments were conducted at a compression ratio range of $\lambda = 10$ to $\lambda = 20$. Two cooling rate protocols were employed for quenching channel die processed samples. Running cold water through the cooling platens provides a cooling rate 0.27°C/s, while running water directly through the channel die cools the polymer sample at a rate of 3.50°C/s. Samples for X-ray measurements were taken from near the ends of the channel die, where the overall strain tensor is predominately tensile along the flow direction (FD), due to the stretching of the block copolymer melt by the flow. In this context, the CD–FD plane is referred to as the "plane of shear" and the FD as the "direction of shear".

2.3. Small angle X-ray scattering analysis

The change in orientation of the resulting microstructure due to deformation was studied by means of SAXS. The SAXS data were obtained using the 10-meter digital camera in the National Institute of Standards and Technology (NIST) Polymers Division [21]. This SAXS instrument is modeled after the one designed by Hendricks [22] at Oak Ridge National Lab. The 2D data sets obtained in these experiments were corrected for dark current and unscattered primary beam. Depending on whether the scattering was isotropic or oriented, the data was reduced to circular or sector averages by averaging over the detector picture elements within a series of annuli located at a fixed
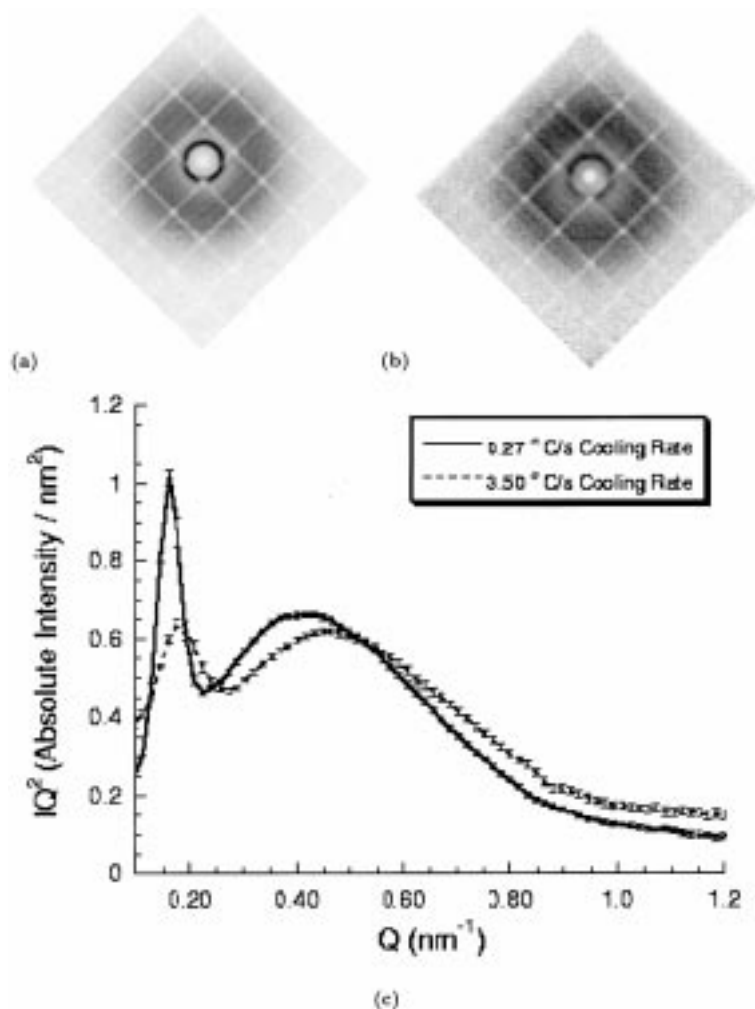
Fig. 2. SAXS pattern of an isotropic triblock cooled at: (a) 0.27°C/s from the melt; (b) 3.50°C/s from the melt; and (c) circular averaged IQ^2 vs Q plots for both cooling protocols.

distance from the beam center. Two sector averages were calculated for oriented samples at azimuthal angles of $\pm 45°$ with a width of $\pm 22.5°$. Sector 1 represents the sector average centered at the constraint direction (CD), while sector 2 refers to the sector average centered at the FD. All intensity values were normalized to a NIST Lupolen sample to provide absolute intensity. Uncertainties were calculated from the standard deviation of the pixel statistics in the averaged annulus and were plotted only when the uncertainty limits were larger than the size of the plotted data points [22,23]. The 2D SAXS patterns are depicted using a linear grayscale colormap representing intensity levels, with darker regions corresponding to higher intensities. The grid pattern seen in the 2D images is the shadow of a support structure that keeps the exit window of the scattered beam path from imploding. Pixels belonging to the grid pattern are masked out of calculations on the 2D patterns.

3. Results

The effect of varying the cooling rate was first explored in isotropic samples. The 2D SAXS pattern obtained for an E/EP/E 30/40/30 isotropic sample which was slow cooled (0.27°C/s) is presented in Fig. 2a and shows two concentric rings. The two peaks obtained for this sample are located at $Q = 0.159 \text{ nm}^{-1}$ for the higher intensity inner ring peak, associated with the microphase separation between the E and EP blocks (B lamellae), and $Q = 0.416 \text{ nm}^{-1}$ for the broader outer ring peak, associated with the crystallization of the E chains (C lamellae). The 2D SAXS pattern for a fast cooled (3.50°C/s) isotropic sample presented in Fig. 2b also shows two concentric rings at similar length scales. The comparison of the IQ^2 vs Q plots for the isotropic slow (Fig. 2c, solid line) and fast (Fig. 2c, dashed line) cooled samples readily shows the changes in morphology produced from the imposition of the faster cooling rate on the semi-crystalline triblock copolymer specimen. The faster cooling

Table 1
Long period spacings of E/EP/E 30/40/30 exhibiting isotropic orientation

Cooling rate (°C/s)	D_1 (nm)	D_2 (nm)
0.27/s	39.3	15.1
3.50	35.7	13.5

rate results in a broader inner ring whose intensity has decreased to nearly equal to the intensity of the outer ring, indicating a lower electron density contrast between the E and EP microphase separated domains. Compared to the slow cooled sample, the inner ring peak location associated with the *B* lamellae has moved to a higher *Q* value of 0.175 nm^{-1}, which is equivalent to a long period spacing decrease of 3.6 nm. The outer ring peak associated with the *C* lamellae has increased in width, in response to the faster cooling rate, while also shifting to a higher *Q* value ($Q = 0.465$ nm^{-1}). The change in long period spacing due to the imposition of the faster cooling rate for the higher *Q* peak is 1.6 nm. The long period spacings obtained for the isotropic samples using the two cooling rates are presented in Table 1.

Channel die plane strain compression processing altered the relationship between microphase separated (*B*)and semi-crystalline (*C*) lamellar populations found in the isotropic E/EP/E triblock copolymer system. Two-dimensional small angle X-ray scattering (SAXS) was used to determine the domain spacing and orientation of the *B* and *C* populations relative to the process directions. The rate at which the channel die assembly was cooled following compression

Fig. 4. SAXS patterns for a fast-cooled triblock exhibiting the C_t microstructure orientation. X-ray beam in: (a) CD; and (b) (FD).

was found to strongly affect the microstructure of the end product. Using a cooling rate of 0.27°C/s, a predominantly perpendicular to the direction of shear orientation of *B* lamellar populations (B_p) is produced, while a cooling rate of 3.50°C/s yields a predominantly transverse to the direction of shear orientation of *C* lamellar populations (C_t).

Increasing the cooling rate from 0.27 to 3.50°C/s during plane strain compression processing above the E block melting point, while applying identical loading conditions, produced a C_t crystalline lamellar microstructure oriented transverse to the direction and normal to the plane of shear. A schematic depiction of the B_p and C_t SAXS patterns and their relationship to the channel die principal deformation directions is shown in Fig. 3. The direction of the normal vector of the C_t lamellae is along the FD, while for the B_p lamellae the normal vector direction is along the CD. An illustration of the parallel, perpendicular and transverse lamellar stacks is also shown in Fig. 3.

The 2D SAXS patterns of the transverse to the direction of shear lamellar microstructure orientation are presented in Figs. 4 and 5. Fig. 5 is the 2D SAXS pattern obtained from irradiating the sample along the loading direction (LD), which shows an arc pattern in the FD corresponding to the C_t long period. When irradiated in the CD (Fig. 4a) spread
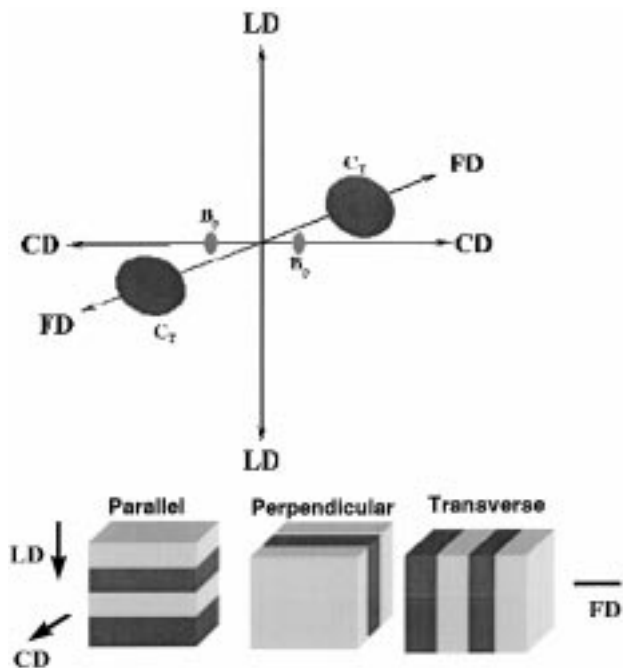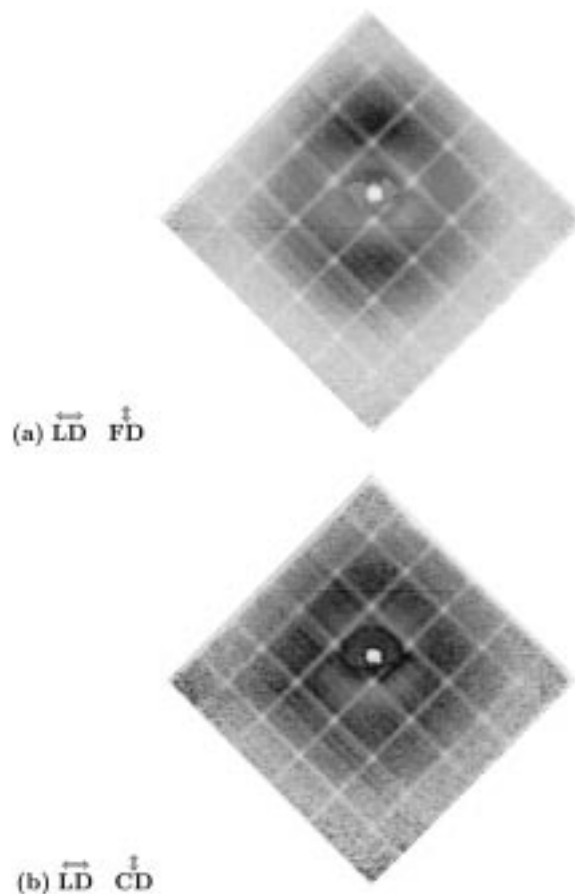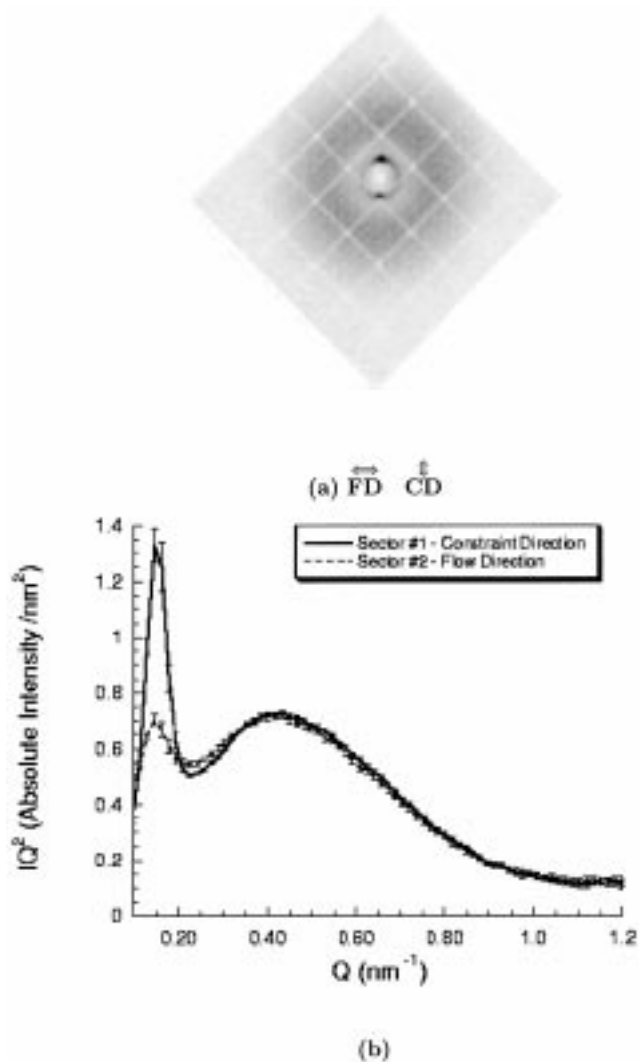

Fig. 3. Schematic of the SAXS patterns for the B_p and C_t microstructures and their relationship to the channel die principal deformation directions in semicrystalline block copolymers.

Fig. 5. (a) LD SAXS pattern; and (b) IQ vs Q plots of the two sector averages of a slow-cooled triblock exhibiting the B_p microstructure orientation along the CD.
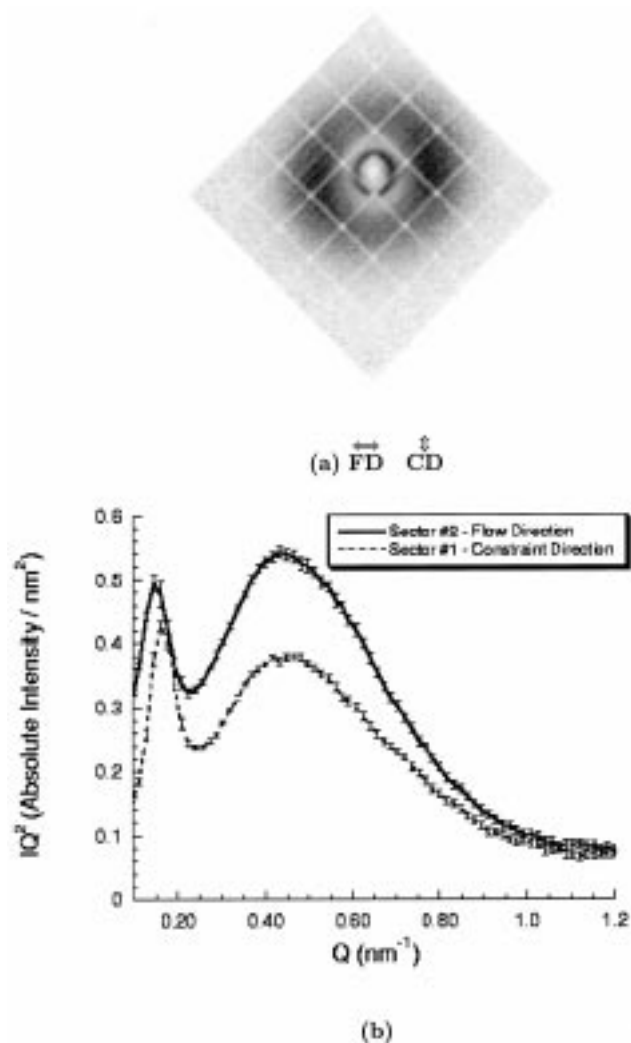

Fig. 6. (a) LD SAXS pattern; and (b) IQ vs Q plots of the two sector averages of a fast-cooled triblock exhibiting the C_t microstructure orientation along the FD.

out spots appear in the FD. The FD SAXS pattern, (Fig. 4b) shows a faint ring pattern. The combined results from these SAXS patterns verify that the transverse to the direction of shear, C_t, is the predominant microstructure orientation of the semicrystalline E lamellae in this sample.

Two-dimensional SAXS patterns and IQ^2 vs Q plots for the two sector averages are presented in Fig. 5 for the perpendicular microphase separated block copolymer lamellar microstructure, B_p, and in Fig. 6 for the transverse semicrystalline lamellar microstructure, C_t. The indicated scattering in these figures is from orienting the X-ray beam parallel to the LD. The B_p SAXS pattern (Fig. 5a) obtained using the slow cooling rate protocol, shows sharp spots in the CD with a long period spacing of $D_1 = 43.6$ nm and a diffuse randomly oriented ring with a long period spacing of $D_2 = 14.5$ nm. The C_t pattern, resulting from

the orientation of semicrystalline E lamellae (Fig. 6a), is obtained using the fast cooling rate protocol, and shows arcs in the CD with a long period spacing of $D_1 = 43.7$ nm and sharp spread-out spots in the FD with a long period spacing of $D_2 = 13.1$ nm. Since the theoretically predicted morphology for this triblock copolymer is lamellar, the peak maximum of a plot of IQ^2 vs Q is used to obtain the long period spacing, D, which accounts for the angular dependence of the form factor scattering from lamellae.

The long period spacings from both sectors averages obtained for the B_p and C_t microstructure orientations are presented in Table 2. The long period, D_1, in the E/EP/E triblock corresponds to the sum of the microphase separated E and EP domain thicknesses, while D_2 is the sum of the crystalline and amorphous regions within the semicrystalline E block. D_1 and D_2 are obtained from the position of the maxima of the two peaks shown on the IQ^2 vs Q plot

Table 2
Long period spacings of perpendicular B_p and transverse C_t microstructure orientations

Cooling rate (°C/s)	D_1 (nm)	D_2 (nm)	Sector average #
Perpendicular orientation texture			
0.27	43.6	14.5	Sector #1-CD
0.27	43.6	14.5	Sector #2-FD
Transverse orientation texture			
3.50	43.7	13.1	Sector #1-CD
3.50	43.6	14.5	Sector #2-FD

Table 3
Percent crystallinity obtained for the oriented morphologies from DSC scans

Cooling rate (°C/s)	Orientation	% Mass crystallinity
0.27	Perpendicular	32
3.50	Transverse	19

using Eq. 1

$$D(\text{nm}) = \frac{2\pi}{Q} \tag{1}$$

The nominal melting point of the crystallizable E block for this E/EP/E copolymer, is 102°C, as determined by a DSC instrument at a heating rate of 10°C/min. The broad melting curve shown in Fig. 7 for this sample indicates the presence of crystals of varying size and perfection. The percent mass crystallinity (Eq. 2) was obtained from the areas of endothermic peaks in DSC graphs (ΔH_f) using a ΔH_f^* value of 69 cal/g for an infinite perfect crystal of polyethylene [6]

$$\text{Mass Crystallinity, } X_c = \frac{\Delta H_f}{\Delta H_f^*} \tag{2}$$

The crystallinity of the B (0.27°C/s) and C (3.50°C/s) microstructures as determined from DSC scans (Table 3), indicates that the sample exhibiting the C_t microstructure orientation has a lower crystallinity than the one showing the B_p orientation. The lower crystallinity in the transverse specimen is the result of the faster cooling rate protocol, which limits the available time for crystal growth.

Annealing of the C_t microstructure was also explored. The transverse sample was annealed below the E block melting point at 70°C for 24 h in a vacuum furnace. The 2D SAXS pattern of the pre-annealed sample is shown in
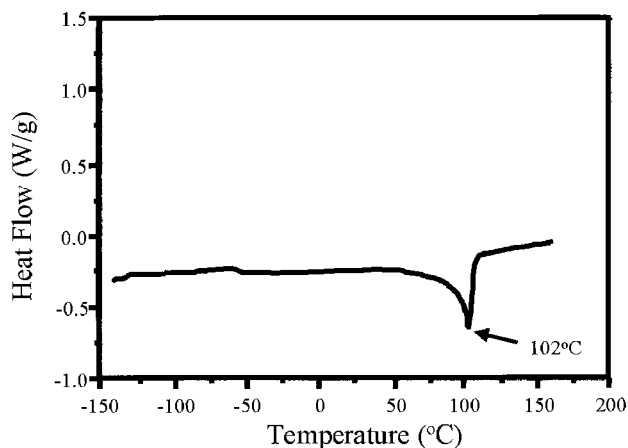
Fig. 8a and the post-annealed sample is shown in Fig. 8b. An improvement in the orientation of the crystals is obtained from the annealing treatment as clearly shown in the sector averaged IQ^2 vs Q plot of the pre-annealed and post-annealed samples compared in Fig. 8c. A significant increase in the peak height associated with the crystallization of the E chains can be seen in the post-annealed sample (solid line) over the pre-annealed sample (dashed line).

Two series of samples were processed using the channel die at a range of temperatures, which were above and within the E block melting point of 102°C, to further investigate the mechanism relating the cooling rate to the microstructure orientation. The temperatures investigated were 100, 150 and 175°C. One series of samples was cooled at 0.27°C/s from the defined temperatures and the other series was cooled at 3.50°C/s starting from the same temperatures. Fig. 9 provides the LD 2D SAXS patterns when cooled at 0.27°C/s. The samples processed at 150°C (Fig. 9b) and 175°C (Fig. 9c) indicate that when plane strain compression processed using the slow cooling protocol at these temperatures the B_p microstructure orientation develops, which is verified on the SAXS pattern by the sharp spots in the CD. However, the C_t microstructure orientation is shown to develop at the 100°C SAXS pattern (Fig. 9a). This is indicated by the spread-out spots, which are found in the FD at higher long period spacings.

Fig. 10 provides the LD 2D SAXS patterns for the same temperature range, but with the samples being processed using the fast cooling rate protocol of 3.50°C/s. The spread out spots, which can be seen in the FD SAXS patterns, show that the C_t morphology develops regardless of the temperature the channel die process commences.

In order to determine the effect of the applied load on the microstructure orientation, the semicrystalline triblock copolymer was heated to 150°C, and a load of 9.2 MPa was applied until the polymer melt began to flow out of the channel die. At this point, the load was released and the sample was immediately quenched at 3.50°C/s to room temperature. This "load-release" SAXS pattern exhibits an isotropic orientation.

4. Discussion

A cooperative interplay between the kinetic process of crystallization and the thermodynamic process of segregation of the blocks apparently leads to the C_t and B_p

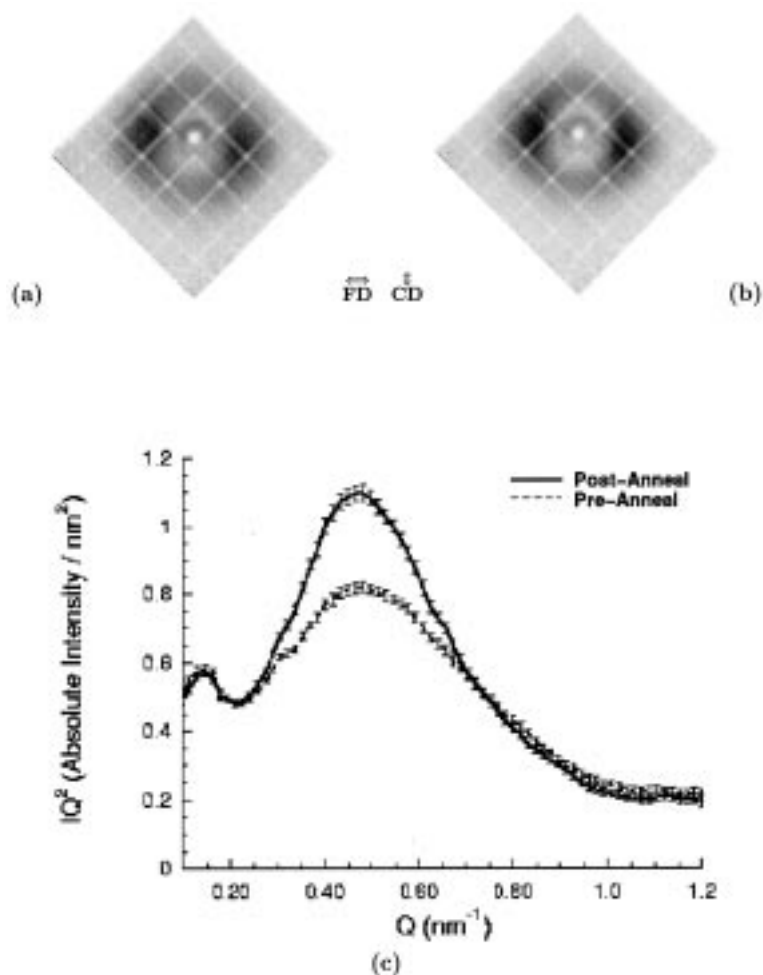Fig. 7. DSC scan for the E/EP/E 30/40/30 triblock heated at 10°C/s.

Fig. 8. LD SAXS patterns of the C_t microstructure orientation: (a) pre-annealed; (b) post-annealed; and (c) the FD sector averaged IQ^2 vs Q plot for the pre-annealed and post-annealed samples.

microstructure orientations observed during plane strain channel die processing of the E/EP/E semicrystalline block copolymer system. In previous investigations [14,15] it was concluded that E/EP diblock and E/EP/E triblock systems form heterogeneous melts under the shear field imposed from the channel die, when deformed at 150°C, which is above the E block melting point. As the E/EP and E/EP/E samples are slow cooled under load, the "perpendicular" microphase separated block copolymer lamellae are frozen-in at the onset of crystallization [14,15], and the crystallization of the E chains occurs within the confinement of this pre-existing microphase separated block copolymer lamellar morphology, a situation which has already been reported [24–26] for other semicrystalline diblock copolymer systems. This process is equivalent to the B_p microstructure in the E/EP/E 30/40/30 sample which has been slow cooled at 0.27°C/s.

The effect of the channel die processing cooling rate on the microstructure orientation development for the E/EP/E semicrystalline system is better understood when related to the sequence of events which occur as the sample is processed and cooled using various cooling protocols. The triblock copolymer processing temperature and loading conditions are identical in producing both B_p and C_t microstructure orientations. The load is maintained as each sample is cooled at the prescribed cooling rate. When slow cooled, at a rate of 0.27°C/s the homogeneous polymer melt first passes through the ODT where the E and EP blocks microphase separate into amorphous lamellar nanodomains due to the incompatibility of the two blocks. The SAXS pattern of this completely amorphous melt (above the E block melting point) is featureless [15], because there is not enough electron density difference between the amorphous E and EP blocks to provide the necessary X-ray contrast. The melt then cools, still under 9.2 MPa of load, through the E block crystallization temperature. Below this temperature, the E block chains crystallize within the confinement of the block copolymer microphase separated domains yielding the frozen-in microstructure observed by SAXS at room temperature. The crystallization of the E block is the reason why any features are observed in the SAXS patterns. The electron density difference between
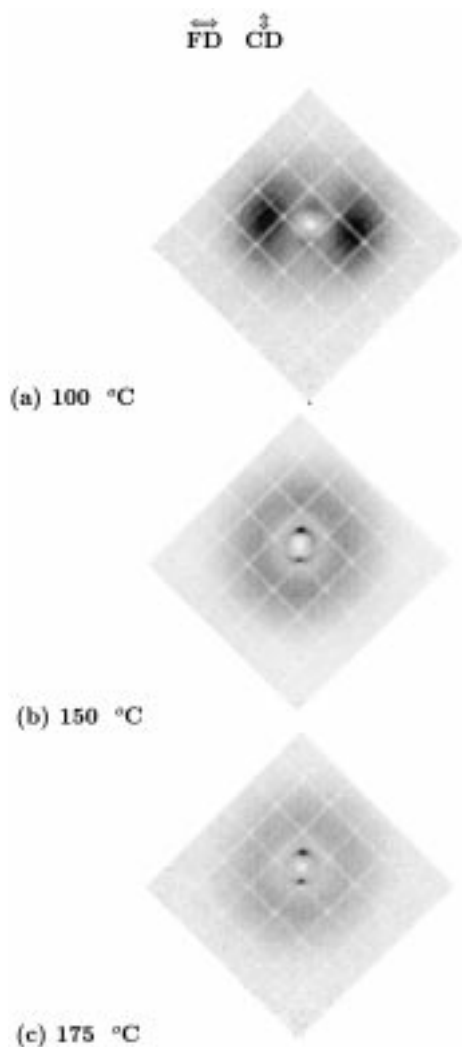
$\overleftrightarrow{FD}$ $\overset{\updownarrow}{CD}$

(a) 100 °C

(b) 150 °C

(c) 175 °C

Fig. 9. LD SAXS patterns: Variations in processing temperatures with identical deformation conditions in slow cooling rate protocol.

$\overleftrightarrow{FD}$ $\overset{\updownarrow}{CD}$

(a) 100 °C

(b) 150 °C

(c) 175 °C

Fig. 10. LD SAXS patterns: Variations in processing temperatures with identical deformation conditions in fast cooling rate protocol.

the semicrystalline E and amorphous EP blocks now provide adequate contrast for features to appear on the SAXS pattern. The long period spacings shown in Table 2 are thus composed of the following: D_1 is the domain thickness of the microphase separated lamellar populations comprised of the E and EP blocks. D_2 is the crystalline long period spacing within the E block. The large intensity of the sharp spots shown on the 2D detector CD pattern in the B_p microstructure in Fig. 5a compared to other regions provides an indication that the relative population of the $D_1 = 43.6$ nm microphase separated lamellar population is the highest. This is verified by the sector #1 (CD) average of this pattern in Fig. 5b where a sharp peak is shown.

The higher cooling rate of 3.50°C/s causes the sample to travel through the ODT and the E block crystallization temperature significantly faster compared to the slow cooling protocol, resulting in a decrease of the final observed crystallinity of the E block. This is supported by the decrease in height of the microphase separated E/EP peak
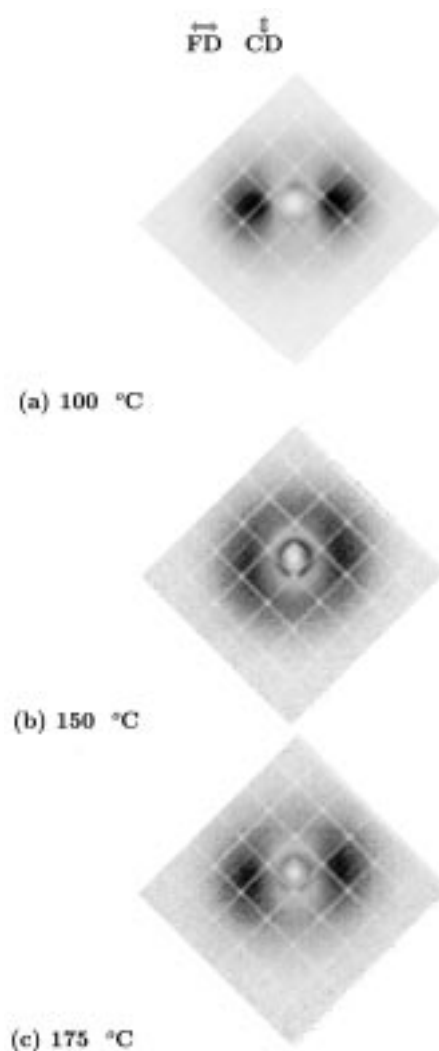
of the fast cooled sample as shown in sector #1 (CD) of Fig. 6b when compared to sector #1 (CD) in the slow cooled sample of Fig. 5b. The lower crystallinity of the fast-cooled sample results in a lower electron density difference between the E and EP blocks compared to the slow-cooled protocol, and thus a lower X-ray contrast. This conclusion has been verified by the SAXS data obtained from Fig. 2 in isotropic samples, which show a lower overall intensity for the fast cooled sample. In addition, the intensity of the inner ring (lower Q value peak) decreases to nearly the same intensity as the outer ring (higher Q value peak). The SAXS patterns from the E/EP/E oriented morphologies present similar findings. The C_t microstructure shown in Fig. 6b has the higher Q value peak (D_2) in sector #2 (FD) dominating the intensity of the pattern (spread out spots in the FD) because the height of the lower Q value peak (D_1) in sector #1 (CD) has significantly decreased. To provide further support, thermal analysis with a DSC was used to determine the difference in crystallinity between the C_t and

B_p microstructures. The DSC results found the crystallinity of the C_t (19% mass crystallinity) to be less than the B_p (32% mass crystallinity) morphology.

It is believed that the continuous application of the 9.2 MPa load to maintain the desired processing conditions deforms the crystallized E chains. This deformation results in the pre-existing E crystalline lamellae to be oriented transverse to the direction and normal to the plane of shear. The load-release experiment reinforces the conclusion that the transverse orientation texture is the result of the application during processing of a load, causing deformation of pre-formed E crystallites since an isotropic orientation texture was found when the triblock was fast-cooled without any externally imposed load.

Plane strain compression deformation studies of semicrystalline homopolymers such as Nylon-6 and low density and high density E using a channel die have been reported [28,29]. These samples were deformed below the melting point of the homopolymer. SAXS data from these studies showed that the channel die induced deformation of the pre-existing crystals resulted in semicrystalline lamellae oriented transverse to direction and normal to the plane of shear. Noting the similarity of the transverse orientation to that reported for other semicrystalline homopolymer systems, this deformation mechanism is suggested as a possible source for the transverse microstructure orientation development in the fast cooled E/EP/E semicrystalline block copolymer systems. The transverse orientation has also been observed in wholly amorphous diblock copolymers [27].

Fig. 9 contains the SAXS patterns for a series of E/EP/E 30/40/30 samples with identical deformation conditions cooled at 0.27°C/s from temperatures of 175, 150 and 100°C. The samples processed at 175 and 150°C, which are above the ODT, yield the B_p morphology. In the 100°C sample, morphology is produced. Here the sample is deformed below the E block T_m, therefore the channel die deforms pre-formed crystallites. Although not a homopolymer, this triblock copolymer appears to deform by a similar mechanism as reported in Refs. [28,29].

Fig. 10 contains the SAXS patterns for a series of E/EP/E 30/40/30 samples with identical deformation conditions cooled at 3.50°C/s from temperatures of 175, 150 and 100°C. All three samples yield the C_t microstructure orientation regardless whether processed above or below the melting point of the E block. These results suggest that plane strain compression applied while using the fast cooling protocol through T_m, orients pre-formed crystallites. The obvious question posed is why does the B_p microphase separated morphology not show the E lamellar domain orientation since both samples see identical loading.

The answer is found in the technique in which the stress is applied. In both cooling rates, identical loading conditions of 9.2 MPa are imposed and maintained by the channel die using a manual standard laboratory press. Variations in the stress applied to the melt occur due to the polymer melt response from the applied load. The 1/2 in. by 1/2 in. polymer melt system, located at the onset of the deformation in the center of the die, flows in response to the applied stress. As the polymer flows along the 6 in. length of the die, an attempt is made to maintain the 9.2 MPa applied stress by manually pumping the hydraulic press to account for the polymer moving along the FD. When the fast cooling protocol is applied, the E chains crystallize within approximately 10 s. As a result of this short period of time needed to lower the sample temperature to 25°C, maintaining the desired 9.2 MPa is difficult, and crystallization occurs while attempting to do so. Thus, any additional stress applied to reach 9.2 MPa, deforms the crystallites which have already formed and orients them transverse to the direction and normal to the plane of shear.

When the slow cooling protocol is applied, the sample crystallizes approximately after 3 min. This allows a long period of time relative to the fast cooling case to manually maintain the desired load. In addition, the rate of polymer flow out of the die decreases steadily as the crystallization temperature is approached. This is a result of the viscosity increasing as the crystallization temperature nears. The high viscosity melt just above the crystallization temperature can maintain the 9.2 MPa applied load. The sample crystallizes under a constant load of 9.2 MPa and no additional load is ever applied to the crystallites.

Annealing the semicrystalline block copolymer below the E crystalline block melting point improves the orientation. A clear improvement of orientation can be seen by the sector averaged IQ^2 vs Q plot of pre- and post-annealed samples presented in Fig. 8. A significant increase in height and a narrowing of the width of the peak represent the improvement in microstructure orientation. The pre-existing crystallites in the sample when annealed below the E block melting point provide the thermal energy to reduce the number of defects and misalignments in the sample and thus improves the overall orientation transverse to the direction and normal to the plane of shear.

5. Summary

The development of a particular microstructure orientation during plane strain compression processing of semicrystalline block copolymers is influenced by the combination of the drive for the blocks to segregate and the ability of one of the blocks to crystallize. SAXS is a powerful tool that helps elucidate this complex process, and quantifies the relationship between the B and C lamellar populations. The contrast in the observed SAXS patterns is produced by the difference in electron density between the amorphous and crystalline domains. By changing simple processing parameters, such as the processing temperature, or the rate of cooling of the specimen under load, one can observe SAXS patterns showing parallel, perpendicular or transverse to the direction of shear microstructure orientations.

The transverse to the direction of shear microstructure orientation, brings to light novel interesting features in the interplay of possible morphologies produced in these systems, which in turn have direct effects on measured properties, such as gas transport.

Acknowledgements

References

[1] Bates FS, Fredrickson GH. Annu Rev Phys Chem 1990;41:525.
[2] Bates FS, Schulz MF, Khandpur AK, Forster S, Rosedale JH, Almdal K, Mortensen K. Faraday Discuss 1994;98:7.
[3] Sakurai K, MacKnight WJ, Lohse DJ, Schulz DN, Sissano JA. Macromolecules 1993;26:3236.
[4] Rangarajan P, Register RA, Fetters LJ. Macromolecules 1993;26:4640.
[5] Rangarajan P, Register RA, Adamson DH, Fetters LJ, Bras W, Naylor S, Ryan AJ. Macromolecules 1995;28:1422.
[6] Wunderlich B, Cormier CM. J Polym Sci 1967;A-2(5):987.
[7] Whitmore MD, Noolandi J. Macromolecules 1988;21:1482.
[8] Polis DL, Winey KL. Macromolecules 1996;29:8180.
[9] Pinhiero B, Hadjuk D, Gruner S, Winey K. Macromolecules 1996;29:1482.
[10] Polis DL, Smith SD, Terrill NJ, Ryan AJ, Morse DC, Winey KI. Macromolecules 1999;32:4668.
[11] Laurer JH, Pinheiro BS, Polis DL, Winey KI. Macromolecules 1999;32:4999.
[12] Cohen RE, Cheng P-L, Douzinas K, Kofinas P, Berney CV. Macromolecules 1990;23:324.
[13] Quiram DJ, Register A, Marchand GR, Adamson DH. Macromolecules 1998;31:4891.
[14] Kofinas P, Cohen RE. Macromolecules 1994;27:3002.
[15] Kofinas P, Cohen RE. Macromolecules 1995;28:336.
[16] Kofinas P, Cohen RE. Polymer 1994;35:1229.
[17] Drzal PL, Halasa AF, Kofinas P. Polymer 2000;41:4671.
[18] Lin L, Argon AS. Macromolecules 1992;25:4011.
[19] Song HH, Argon AS, Cohen RE. Macromolecules 1990;23:870.
[20] Halasa AF. US Patent 3 872 072.
[21] Barnes JD, Mopsik F. 46th Annual Technical Conf Proc Soc of Plastics Engineers, vol. 1179, 1988. p. 12.
[22] Hendricks RW. J Appl Cryst 1978;11:15.
[23] Prask HJ, Rowe M, Rush JJ, Schroeder IJ. J Res Natl Inst Stand Tech 1993;8:1.
[24] Douzinas KC, Cohen RE, Halasa AF. Macromolecules 1991;24:4457.
[25] Douzinas KC, Cohen RE. Macromolecules 1992;25:5030.
[26] Cohen RE, Bellare A, Drzewinski MA. Macromolecules 1994;27:2321.
[27] Wiesner U. Makromol Chem Phys 1997;198:3319.
[28] Galeski A, Argon AS, Cohen RE. Macromolecules 1991;24:3953.
[29] Galeski A, Argon AS, Cohen RE. Macromolecules 1992;25:5705.